Supporting information:

Strategies for Switching the Mechanism of Proton-Coupled Electron Transfer Reactions Illustrated by Mechanistic Zone Diagrams

Robin Tyburski, Leif Hammarström*

Department of Chemistry – Ångström Laboratory, Uppsala University, Box 532, SE75120 Uppsala, Sweden.

Contents

S1. Determination of association constants

In order to obtain more accurate estimates of the hydrogen bond association constants (K_{HB}), we made use of its increase with decreasing temperature. Rate constants for oxidation of 4-MeOPhenol by $Ru(dmb)_3^{3+}$ were measured with varying base concentrations at temperatures ranging from 2°C to 22°C. A regression to:

$$k_{obs} = k_{ox}[4-MeOPhenol] = \left(k_{ET(PT)} + k_{CEPT}\frac{K_{HB}[B]}{1 + K_{HB}[B]}\right)[4-MeOPhenol]$$

(eq 8 in themain manuscript), keeping [4-MeOPhenol] constant and varying the base concentration, yielded values for K_{HB}. The natural logarithm of K_{HB} was plotted against 1/T. According to the van't Hoff equation, the natural logarithm of KHB should vary linearly with 1/T following:

$$\ln(K_{HB}) = \frac{\Delta H^0_{HB}}{RT} + \frac{\Delta S^0_{HB}}{R}$$

A linear regression was performed and Hydrogen bond association constants at 22°C were obtained by interpolation.

S1.1 Association constants for 4-methoxypyridine

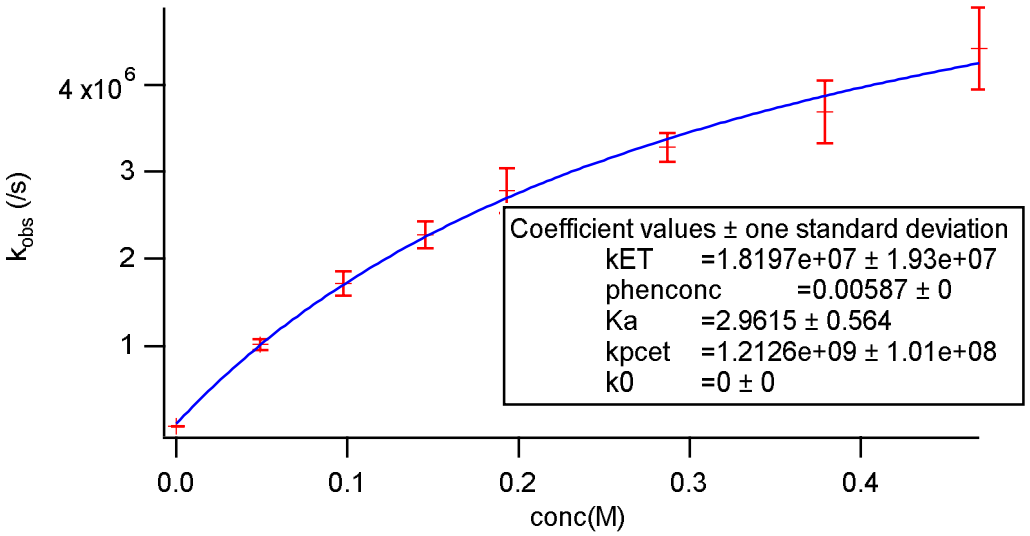

Fig S1.1.1 – Observed rate constants as a function of base concentration at 2°C

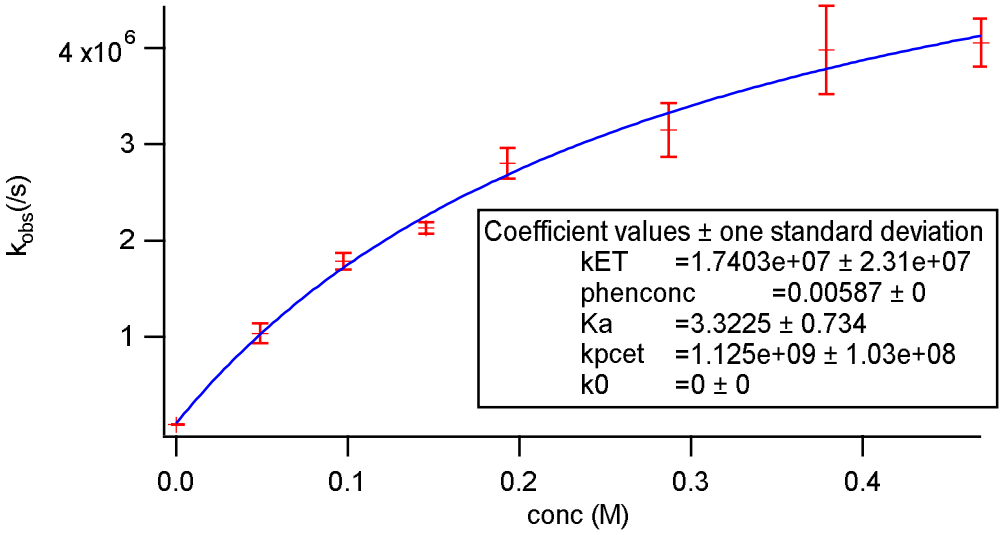

Fig S1.1.2 – Observed rate constants as a function of base concentration at 7°C

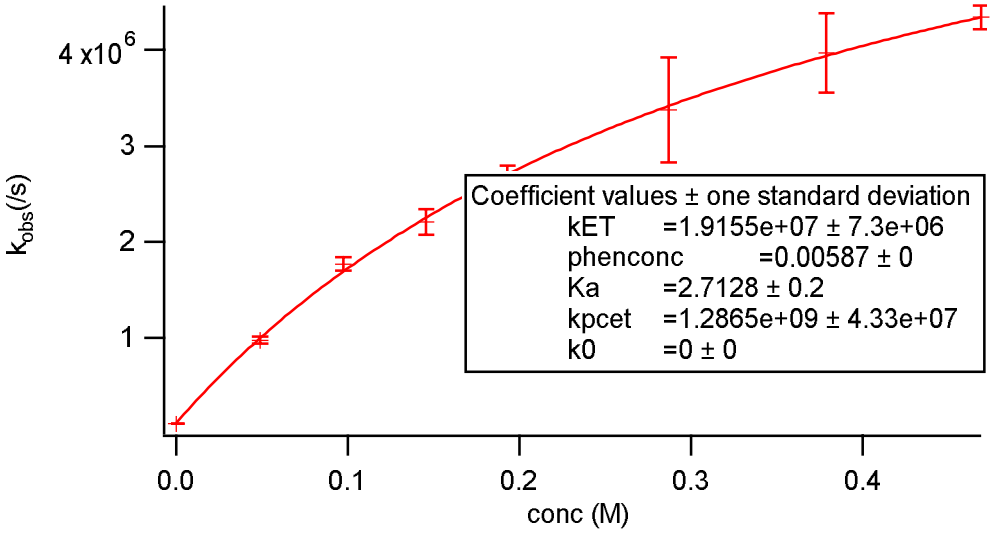

Fig S1.1.3 – Observed rate constants as a function of base concentration at 12°C

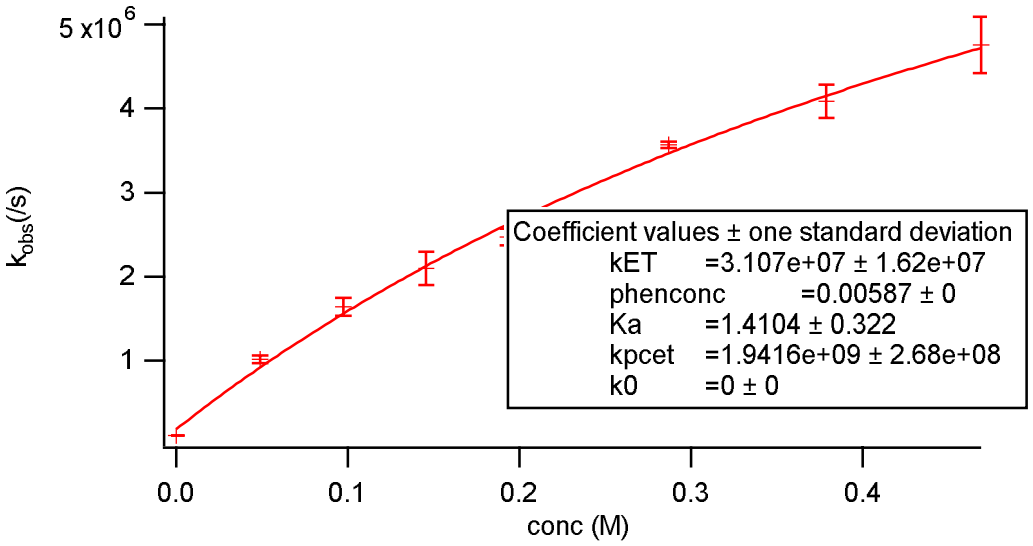

Fig S1.1.4 – Observed rate constants as a function of base concentration at 17°C

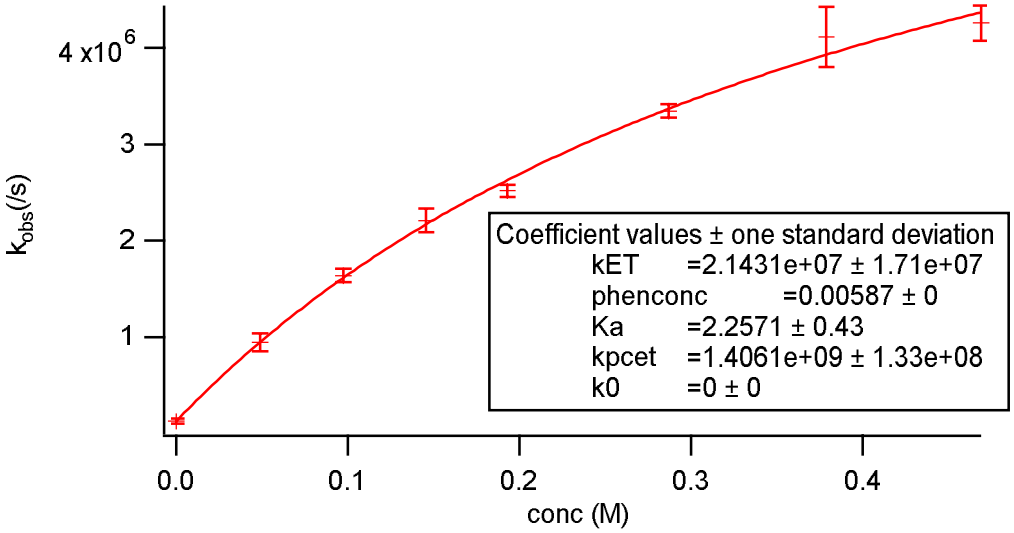

Fig S1.1.5 – Observed rate constants as a function of base concentration at 22°C

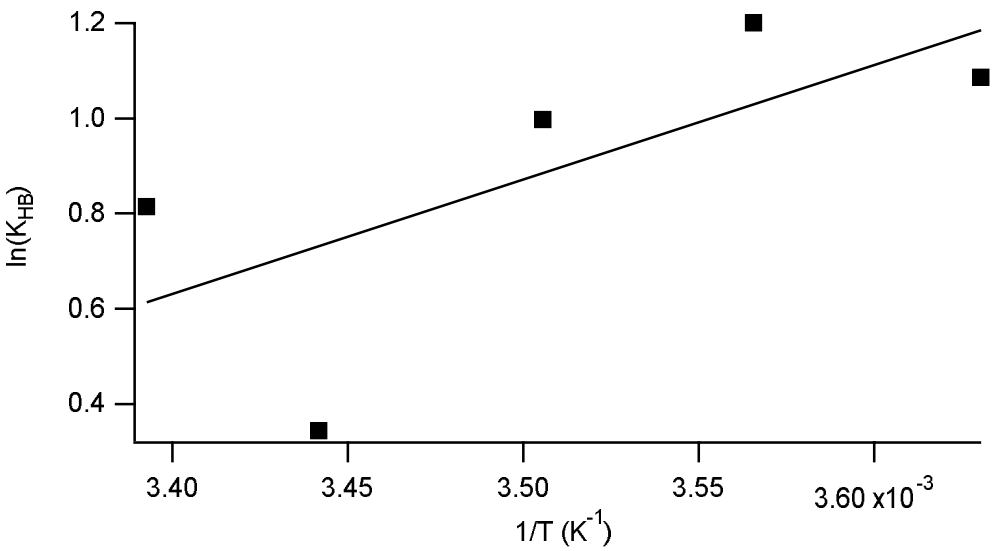

Fig S1.1.6 – Dependence of $\ln(K_{HB})$ on 1/T. K_{HB} at 22°C = 1.85

S1.2 Association constants for pyridine

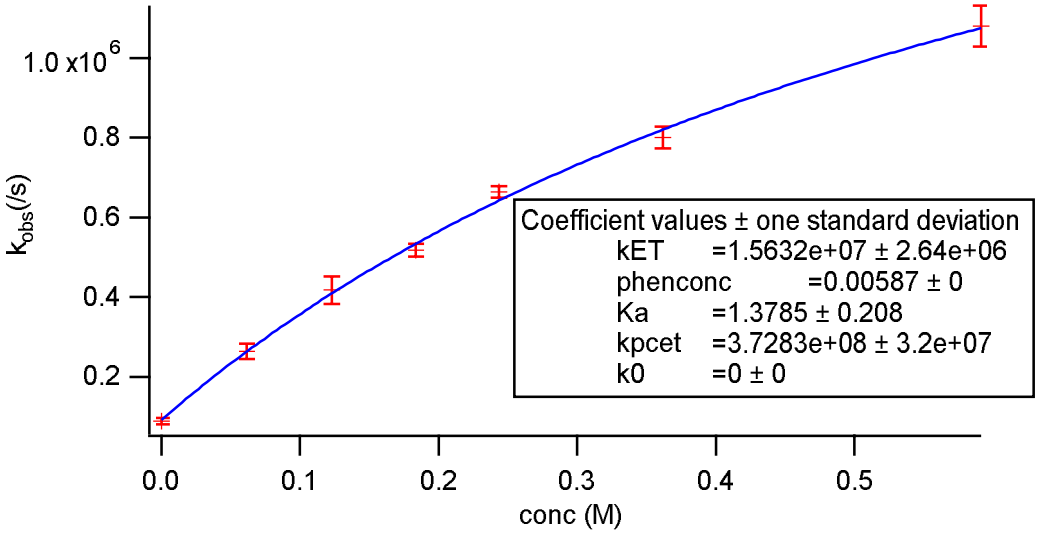

Fig S1.2.1 – Observed rate constants as a function of base concentration at 2°C

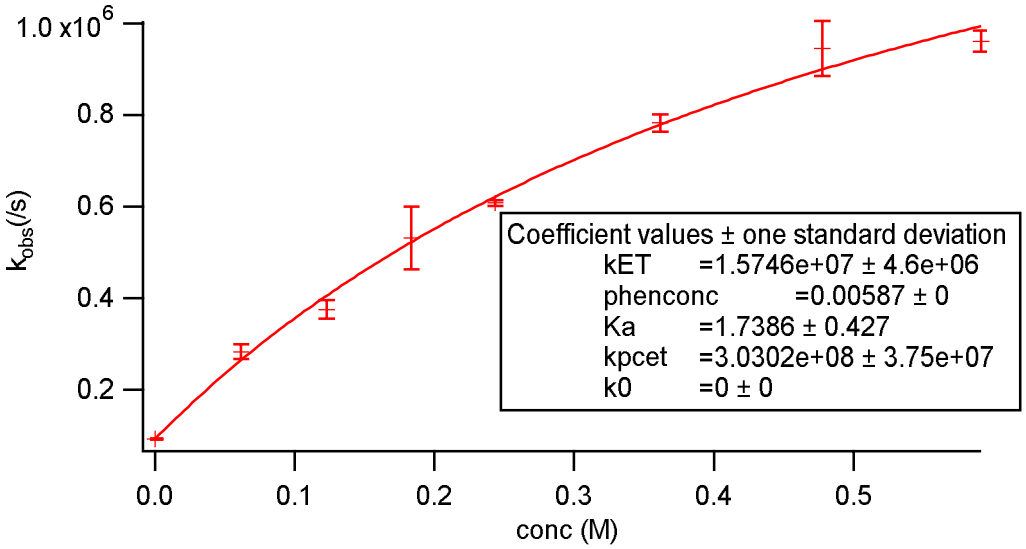

Fig S1.2.2 – Observed rate constants as a function of base concentration at 7°C

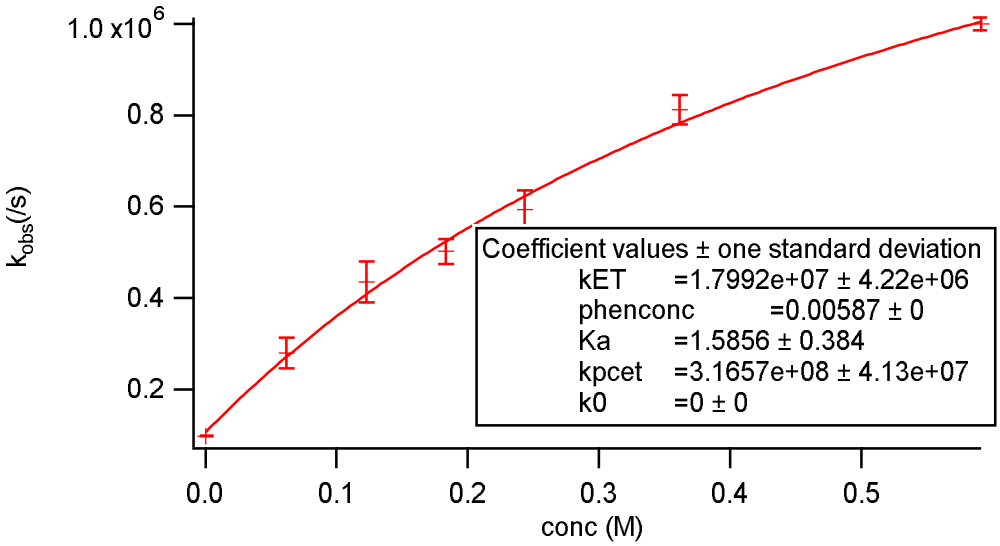

Fig S1.2.3– Observed rate constants as a function of base concentration at 12°C

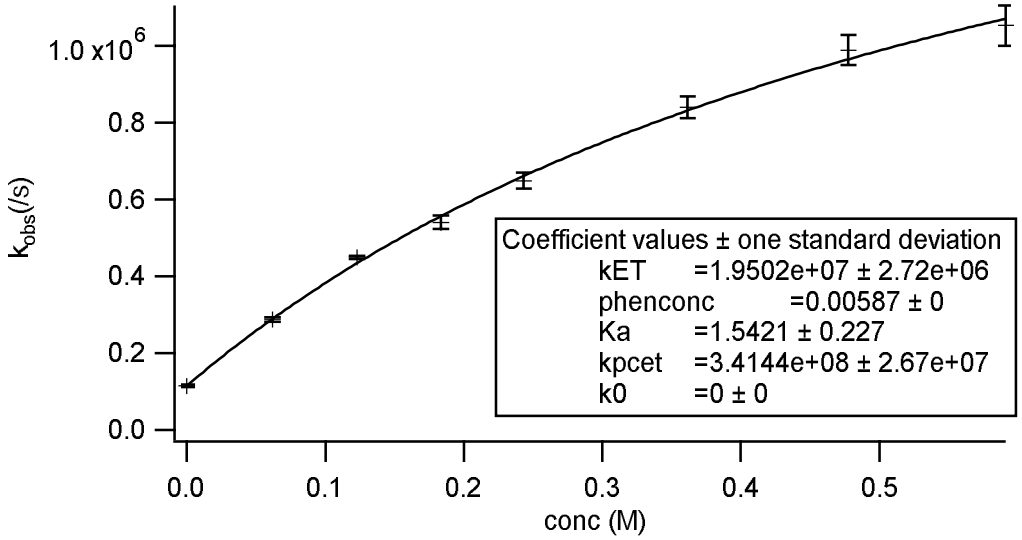

Fig S1.2.4 – Observed rate constants as a function of base concentration at 17°C

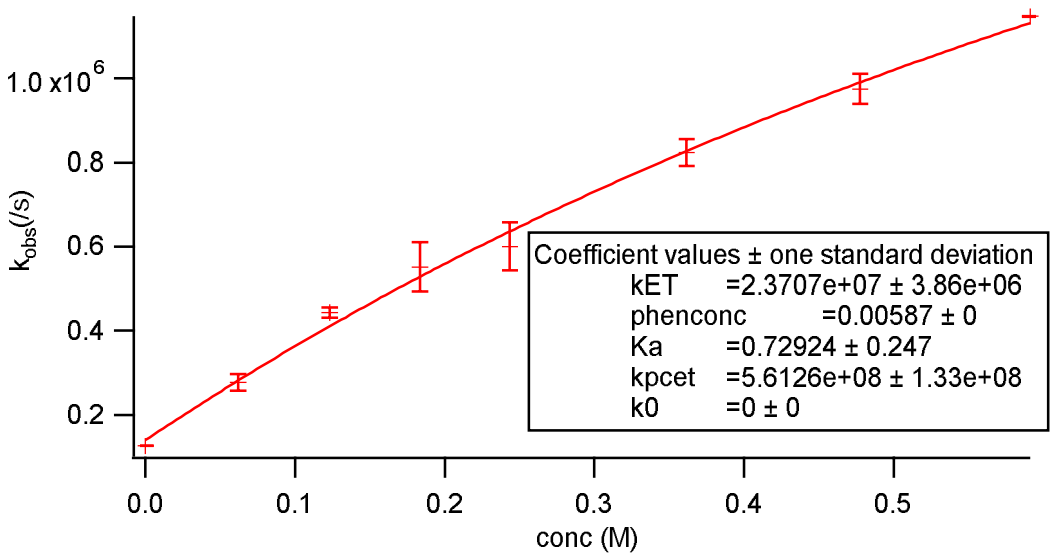

Fig S1.2.5 – Observed rate constants as a function of base concentration at 22°C

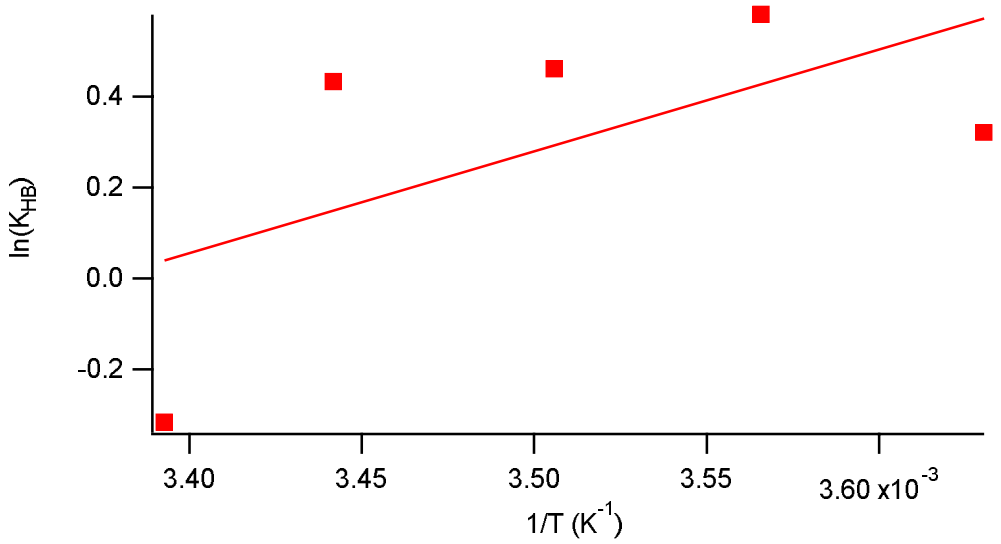

Fig S1.2.6 – Dependence of ln(K_{HB}) on 1/T. K_{HB} at 22°C = 1.04

S1.3 Association constants for 2,6-Lutidine

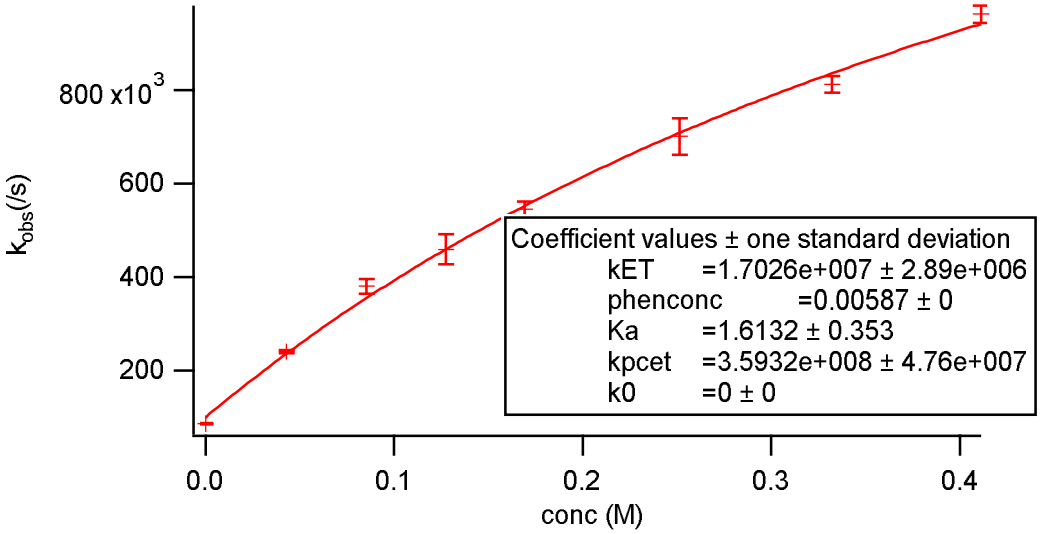

Fig S1.3.1 – Observed rate constants as a function of base concentration at 2°C

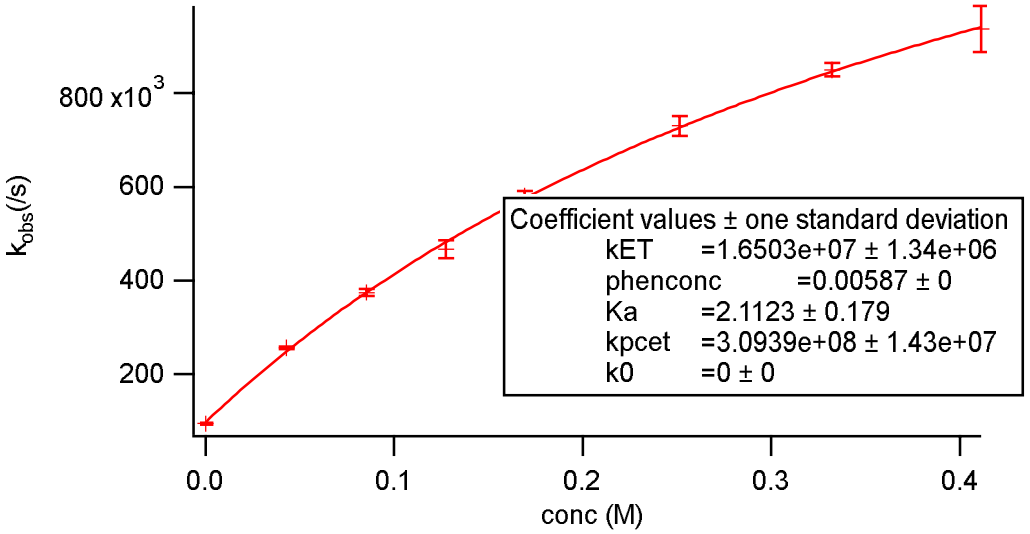

Fig S1.3.2 – Observed rate constants as a function of base concentration at 7°C

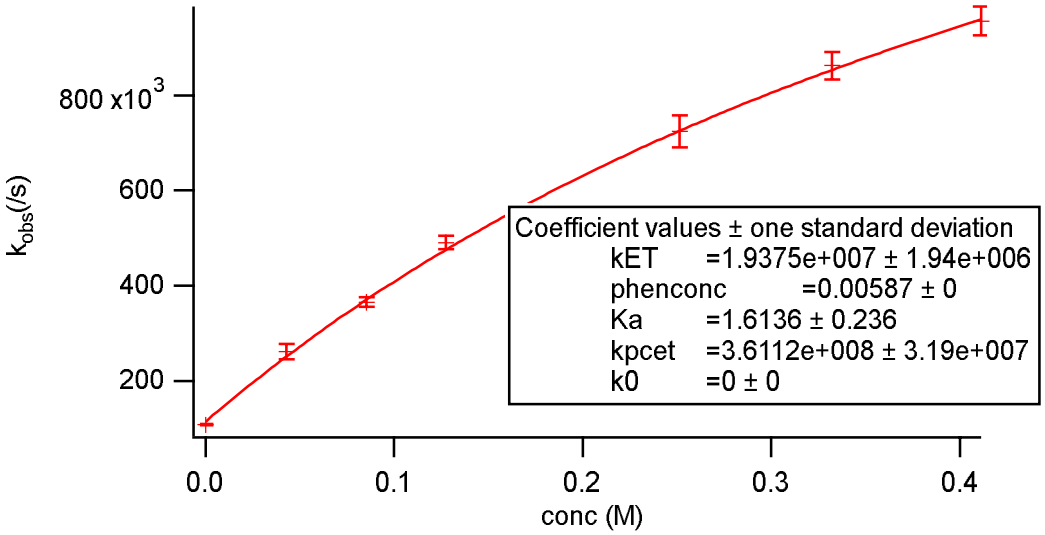

Fig S1.3.3– Observed rate constants as a function of base concentration at 12°C

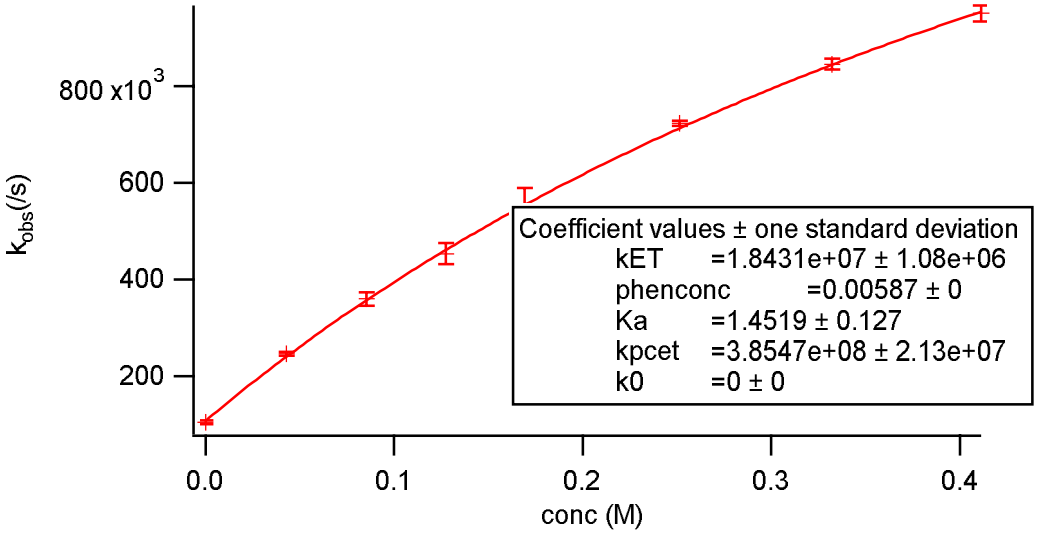

Fig S1.3.4 – Observed rate constants as a function of base concentration at 17°C

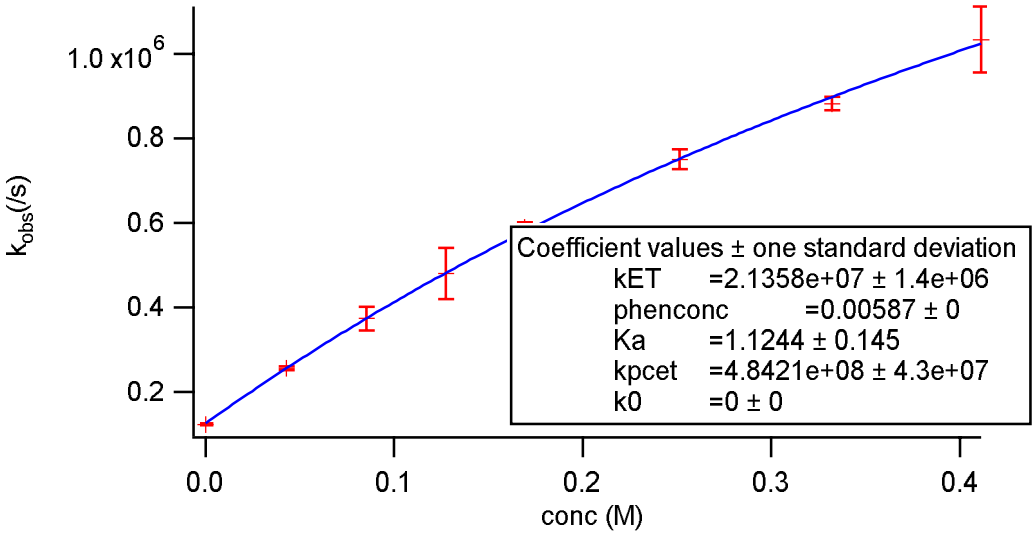

Fig S1.3.5 – Observed rate constants as a function of base concentration at 22°C

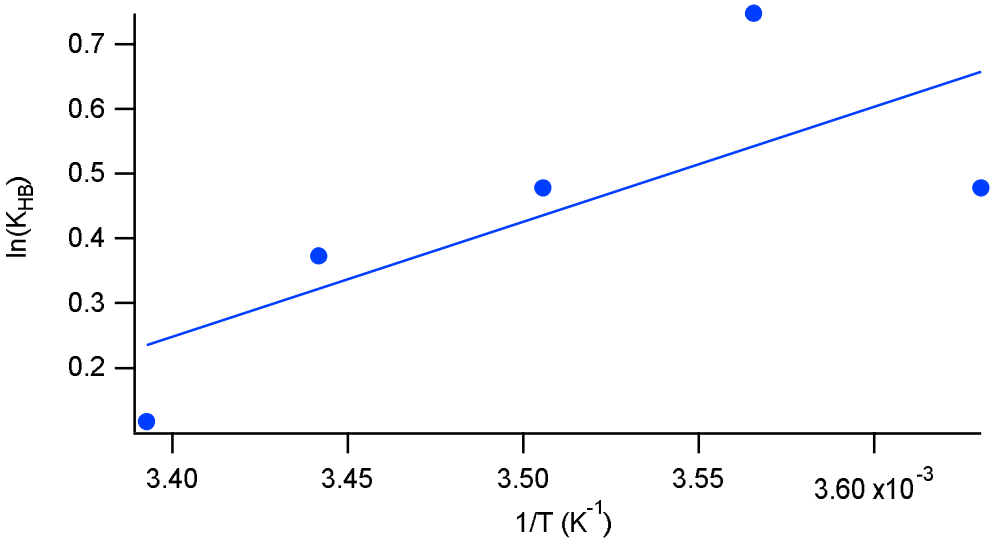

Fig S1.3.6 – Dependence of ln(K_{HB}) on 1/T. K_{HB} at 22°C = 1.26

S1.4 Association constant for 2,4,6-collidine

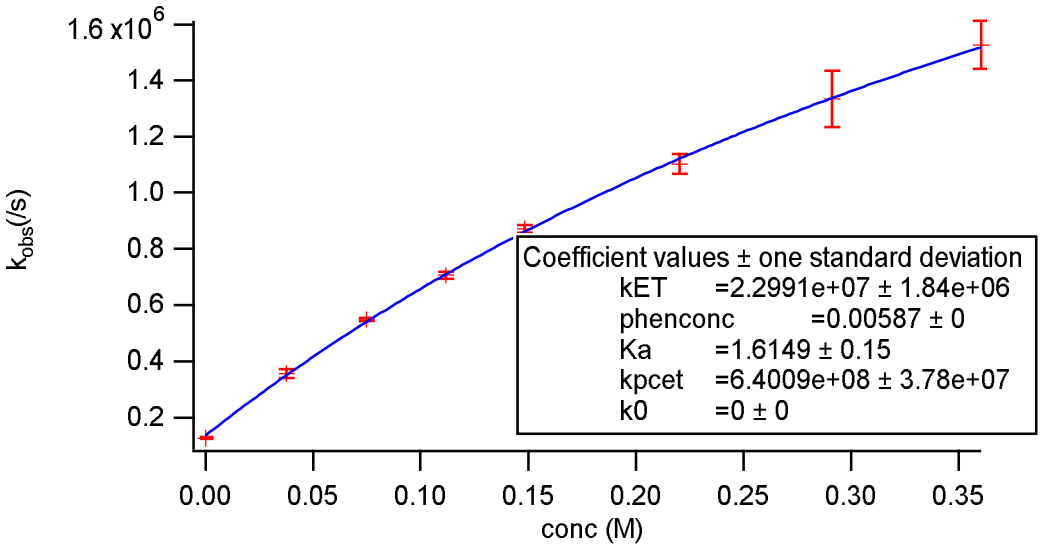

Fig S1.4.1 – Observed rate constants as a function of base concentration at 22°C

S2 Rate constants

Rate constants were obtained by following the regeneration of Ru(II), after flash-quench generation of the Ru(III) oxidant, through monitoring the change in absorption at 450 nm (see experimental section in the main manuscript). Observed rate constants were obtained through single exponential fits. The observed rate constants were plotted as a function of base concentration, and k_{CEPT} was extracted by regression to equation 8 (keeping K_{HB} fixed to the values determined in section S1).

S2.1 Rate constants with 4-Methoxypyridine

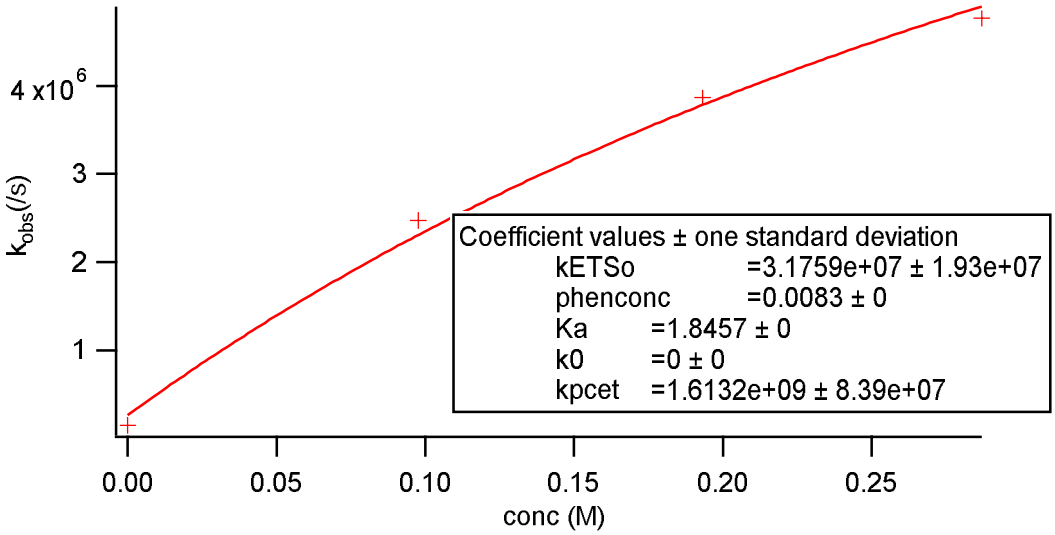

Figure S2.1.1: Observer rate constants for oxidation with $Ru(dmb)_3^{3+}$ as a function of base concentration

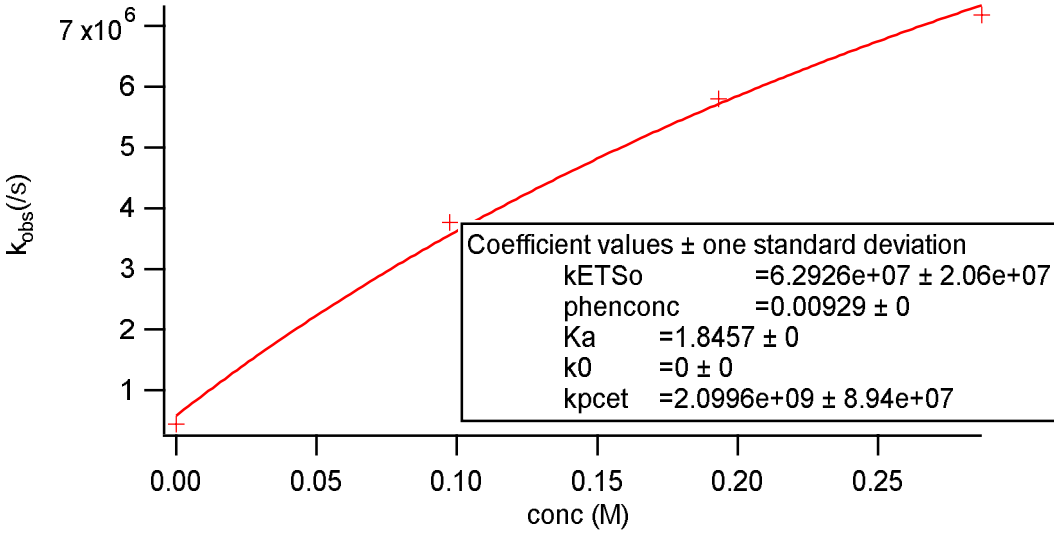

Figure S2.1.2: Observer rate constants for oxidation with $Ru(dmb)_2(bpy)^{3+}$ as a function of base concentration

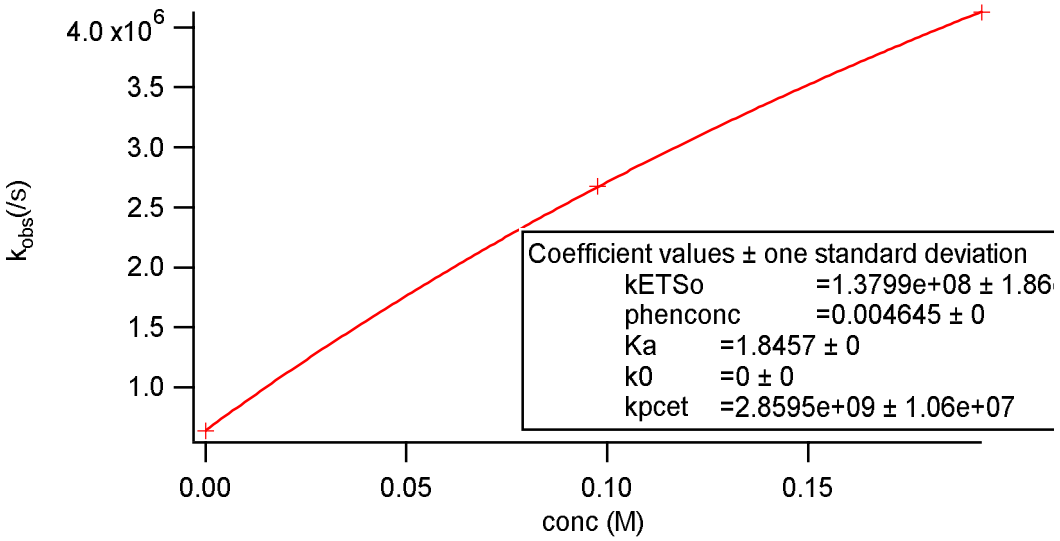

Figure S2.1.3: Observer rate constants for oxidation with $Ru(bpy)_2(dmb)^{3+}$ as a function of base concentration

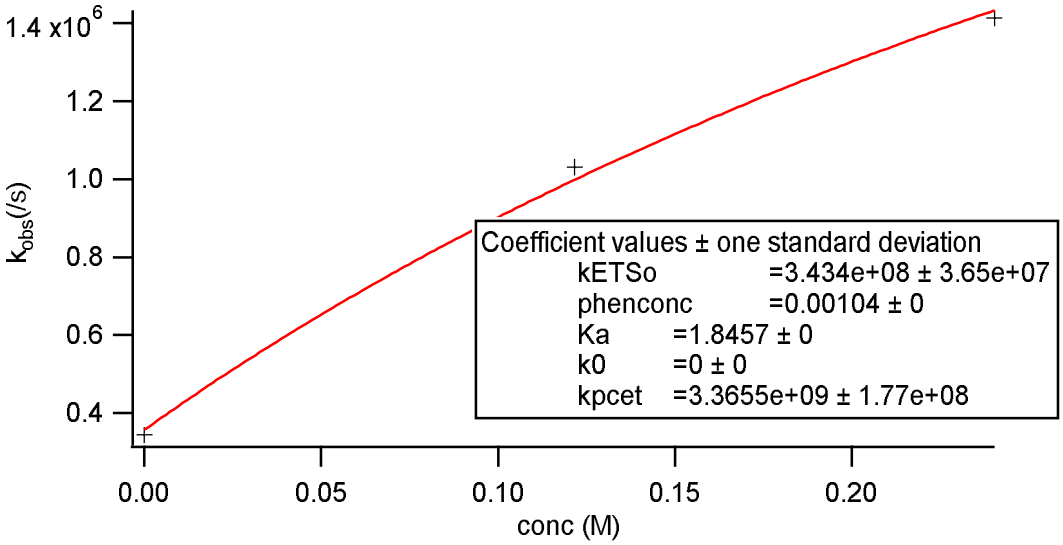

Figure S2.1.4: Observer rate constants for oxidation with $Ru(bpy)_3^{3+}$ as a function of base concentration

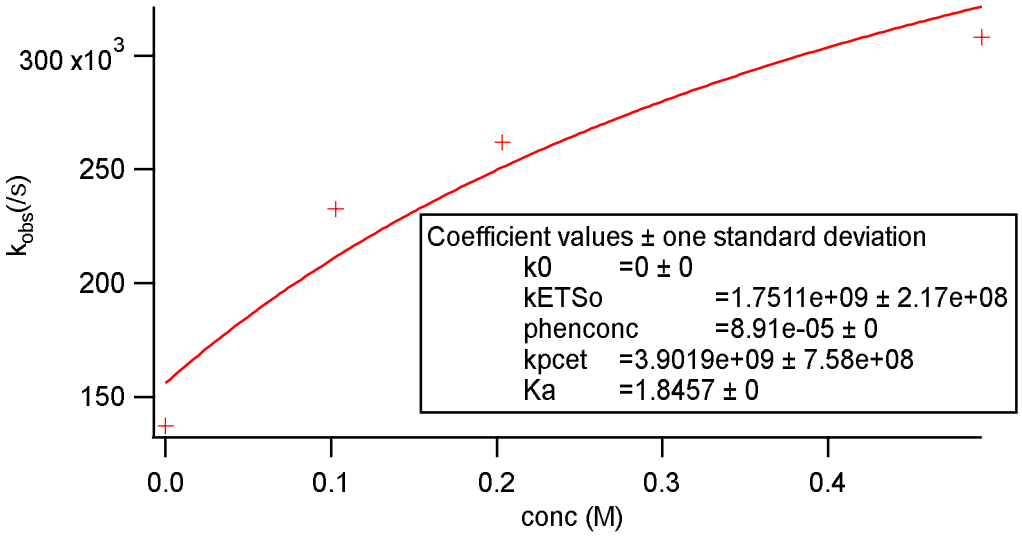

Figure S2.1.5: Observer rate constants for oxidation with $Ru(bpy)_2(deeb)_3^{3+}$ as a function of base concentration

S2.2 Rate constants with pyridine

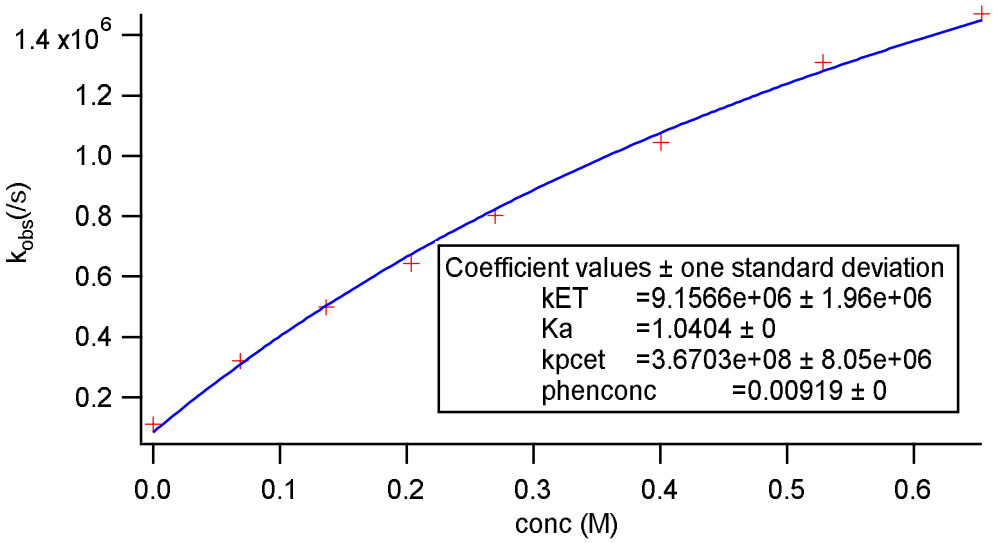

Figure S2.2.1: Observer rate constants for oxidation with $Ru(dmb)_3^{3+}$ as a function of base concentration

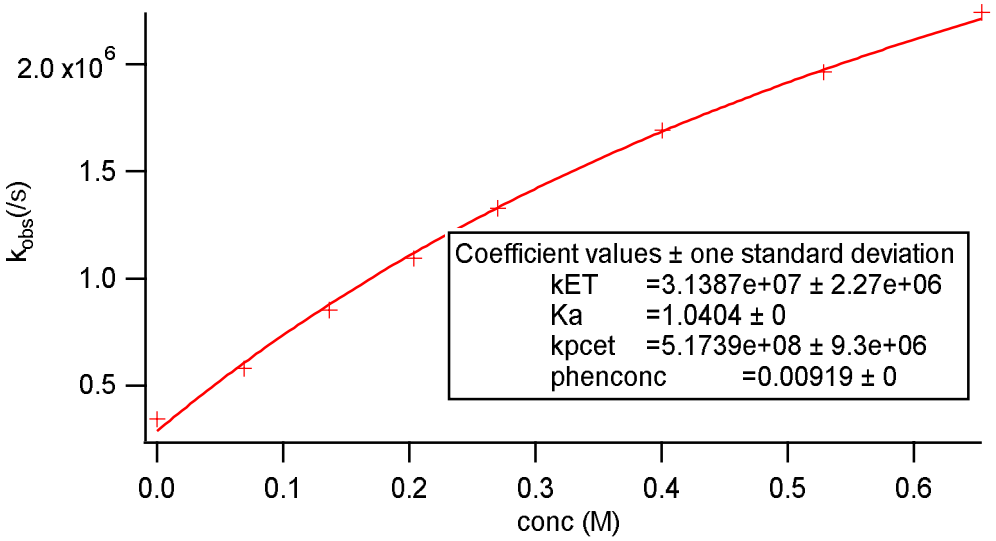

Figure S2.2.2: Observer rate constants for oxidation with $Ru(dmb)_2(bpy)^{3+}$ as a function of base concentration

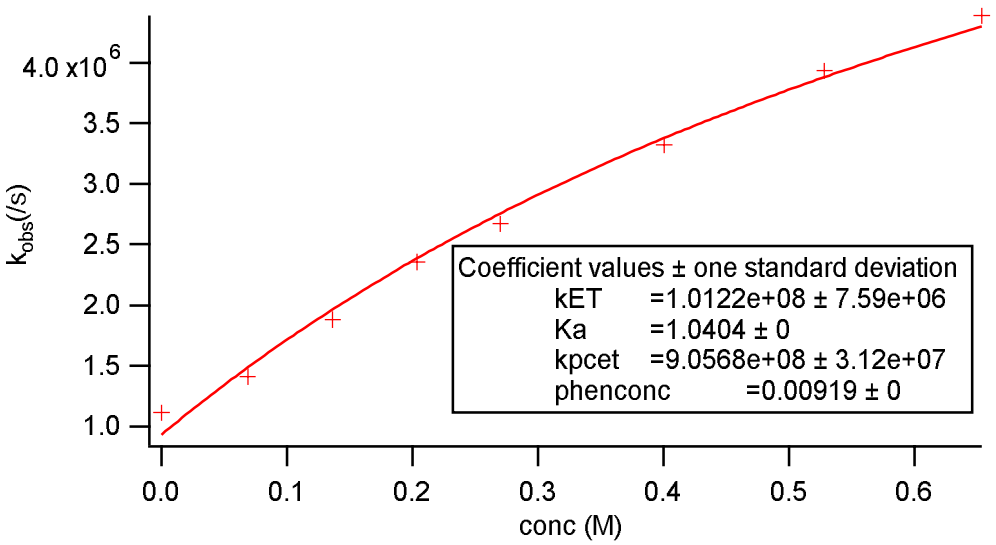

Figure S2.2.3: Observer rate constants for oxidation with $Ru(bpy)_2(dmb)^{3+}$ as a function of base concentration

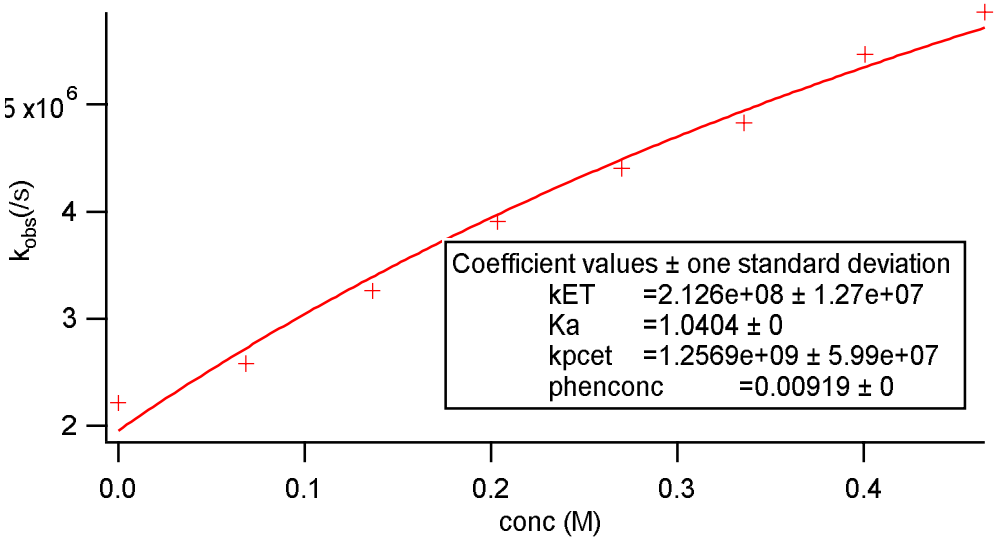

Figure S2.2.4: Observer rate constants for oxidation with $Ru(bpy)_3^{3+}$ as a function of base concentration

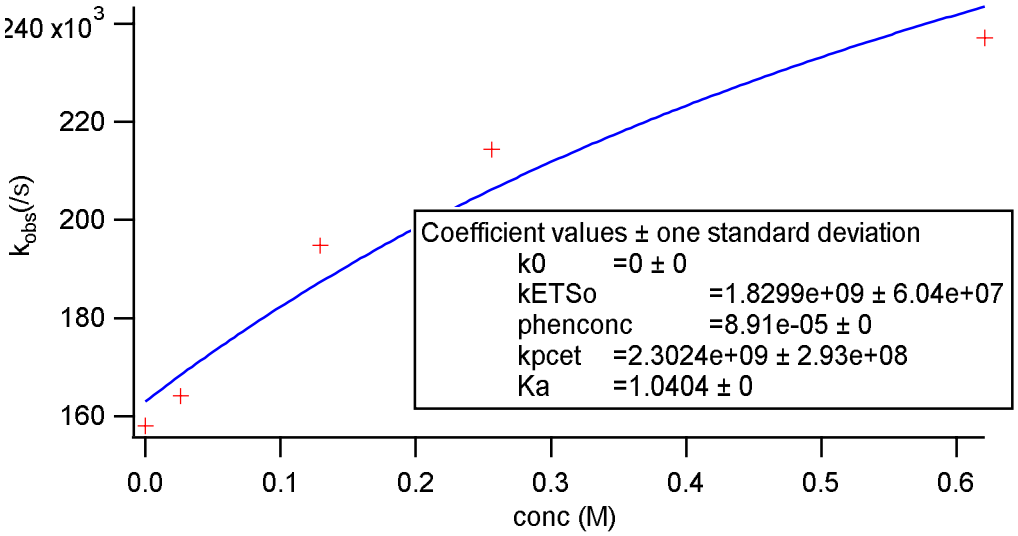

Figure S2.2.5: Observer rate constants for oxidation with $Ru(bpy)_2(deeb)^{3+}$ as a function of base concentration

S2.3 Rate constants with 2,6-Lutidine

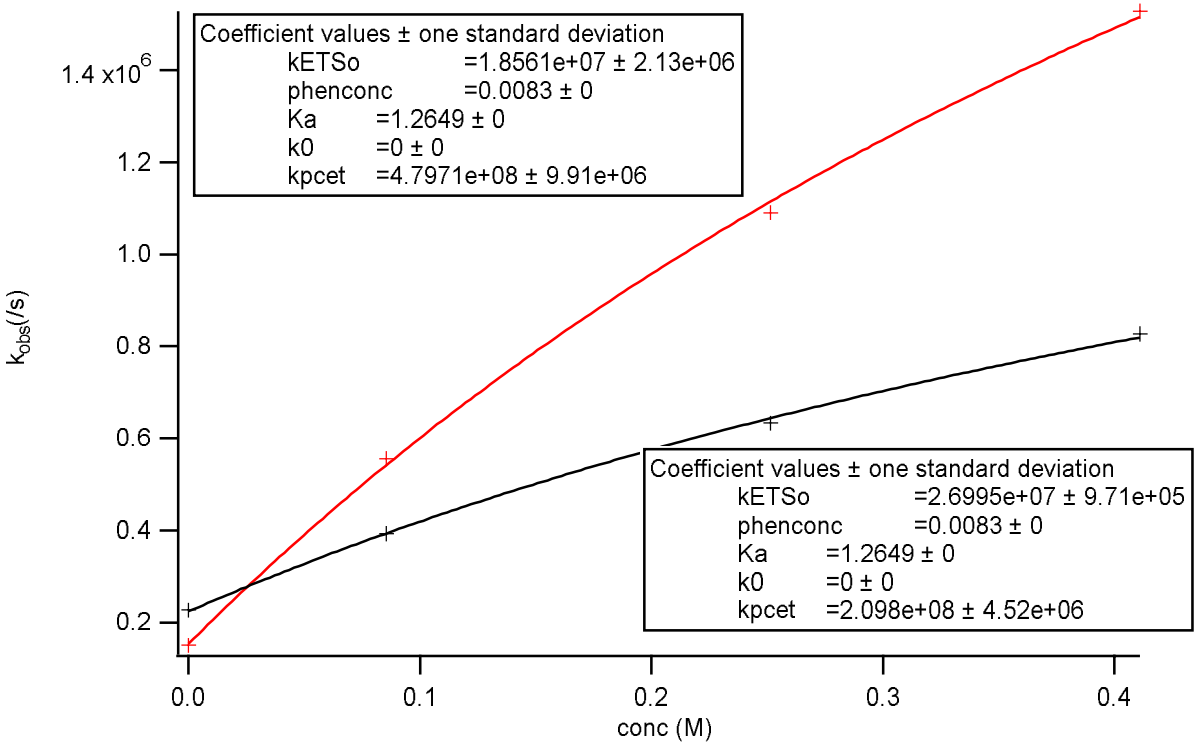

Figure S2.3.1: Observer rate constants for oxidation with $Ru(dmb)_3^{3+}$ as a function of base concentration with (black) and without (red) addition of 1% v/v D_2O

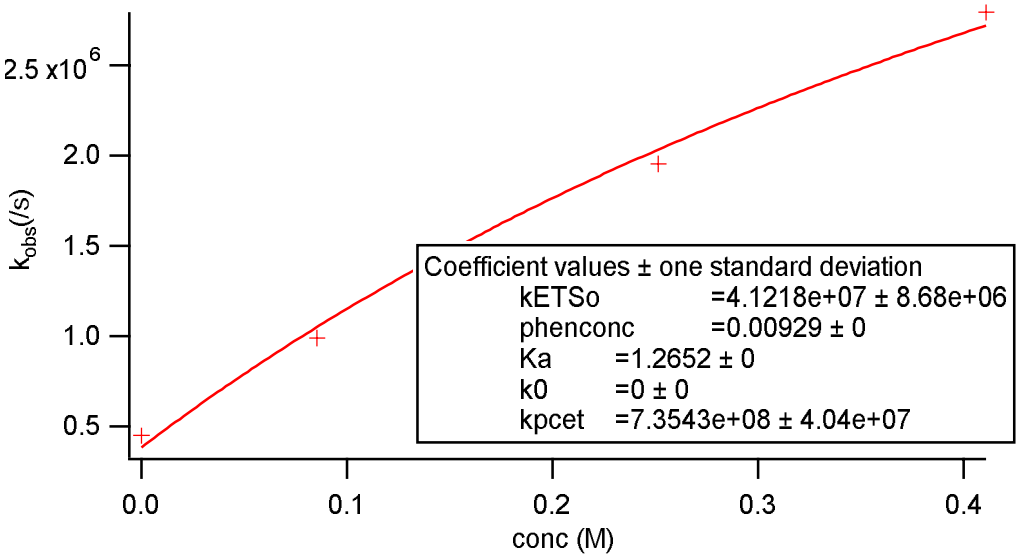

Figure S2.3.2: Observer rate constants for oxidation with $Ru(dmb)_2(bpy)^{3+}$ as a function of base concentration

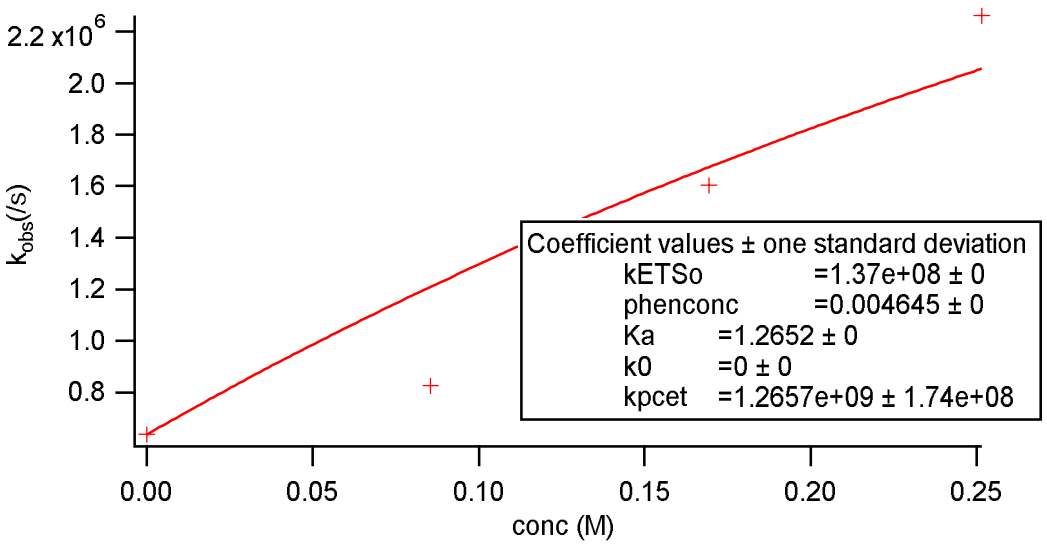

Figure S2.3.3: Observer rate constants for oxidation with $Ru(bpy)_2(dmb)^{3+}$ as a function of base concentration

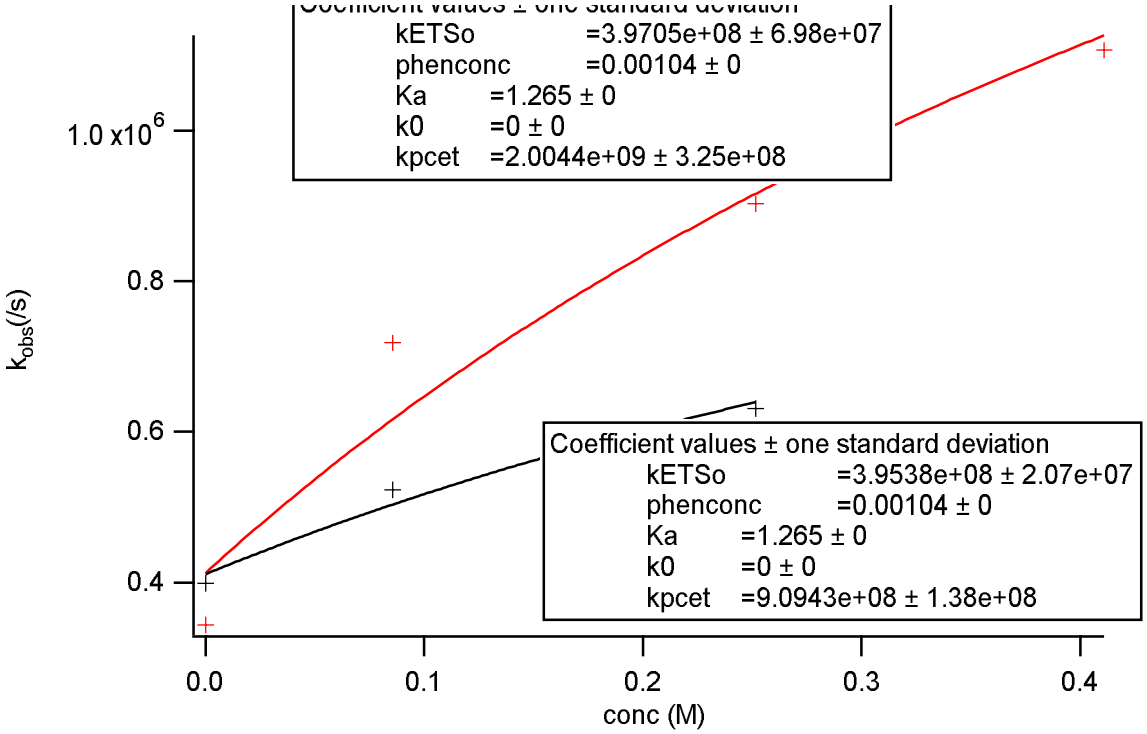

Figure S2.3.4: Observer rate constants for oxidation with $Ru(bpy)_3^{3+}$ as a function of base concentration with (black) and without (red) addition of 1% v/v D_2O

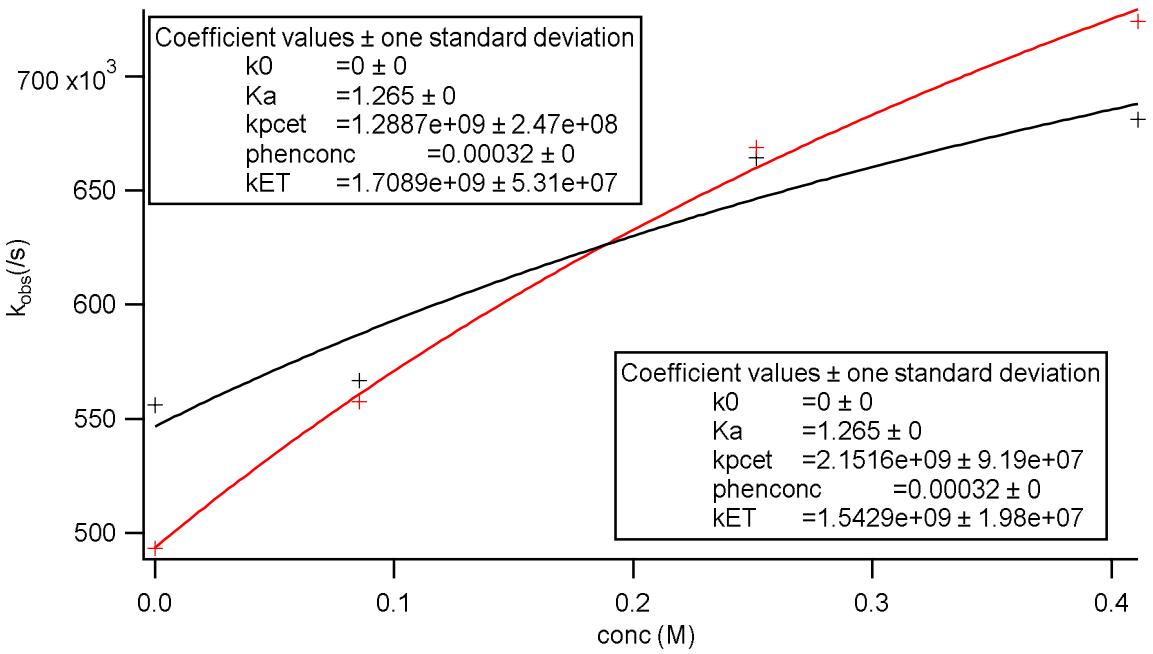

Figure S2.3.5: Observer rate constants for oxidation with $Ru(bpy)_2(deeb)^{3+}$ as a function of base concentration with (black) and without (red) addition of 1% v/v D_2O

S2.4 Rate constants with 2,4,6-collidine

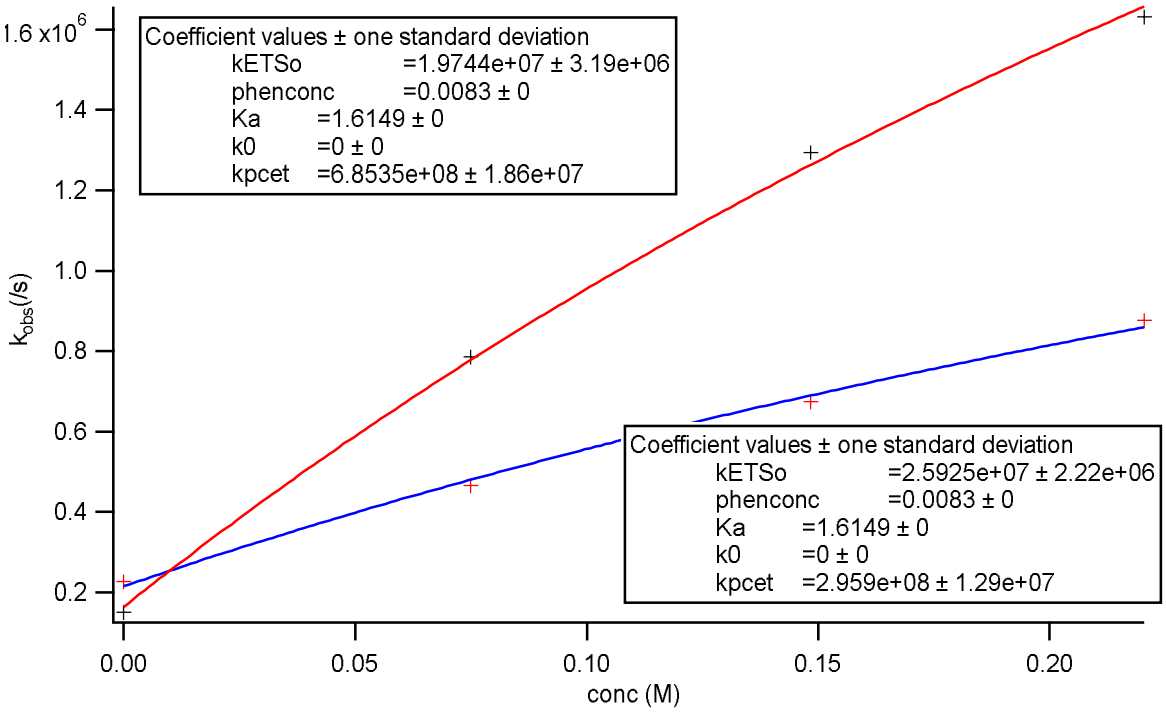

Figure S2.4.1: Observer rate constants for oxidation with $Ru(dmb)_3^{3+}$ as a function of base concentration with (blue) and without (red) addition of 1% v/v D_2O

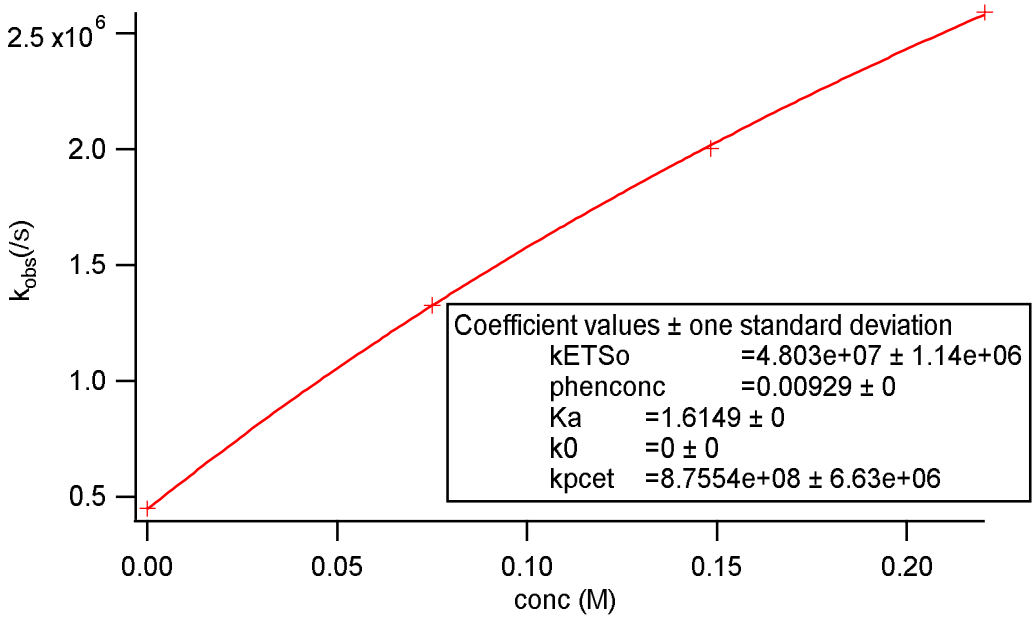

Figure S2.4.2: Observer rate constants for oxidation with $Ru(dmb)_2(bpy)^{3+}$ as a function of base concentration

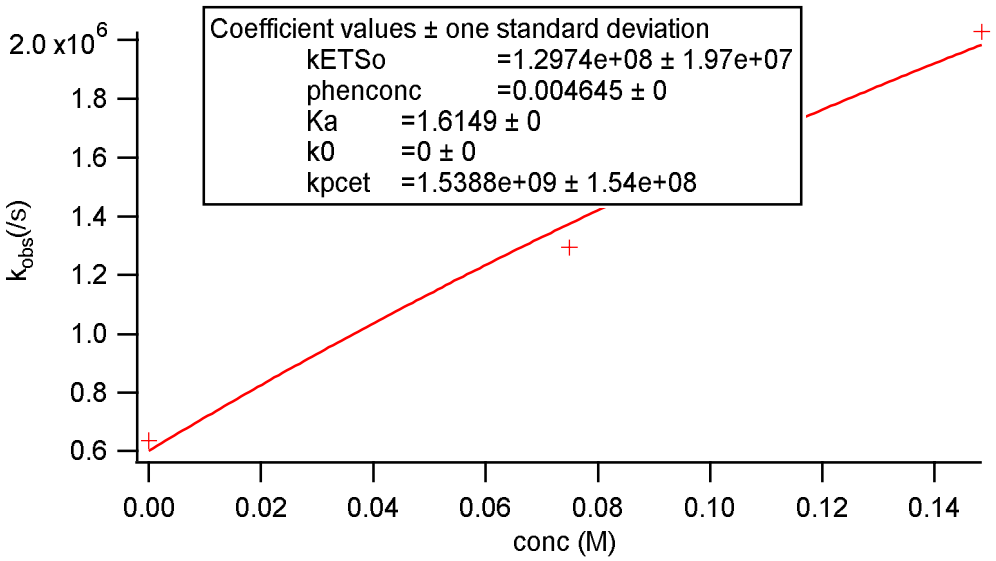

Figure S2.4.3: Observer rate constants for oxidation with $Ru(bpy)_2(dmb)^{3+}$ as a function of base concentration

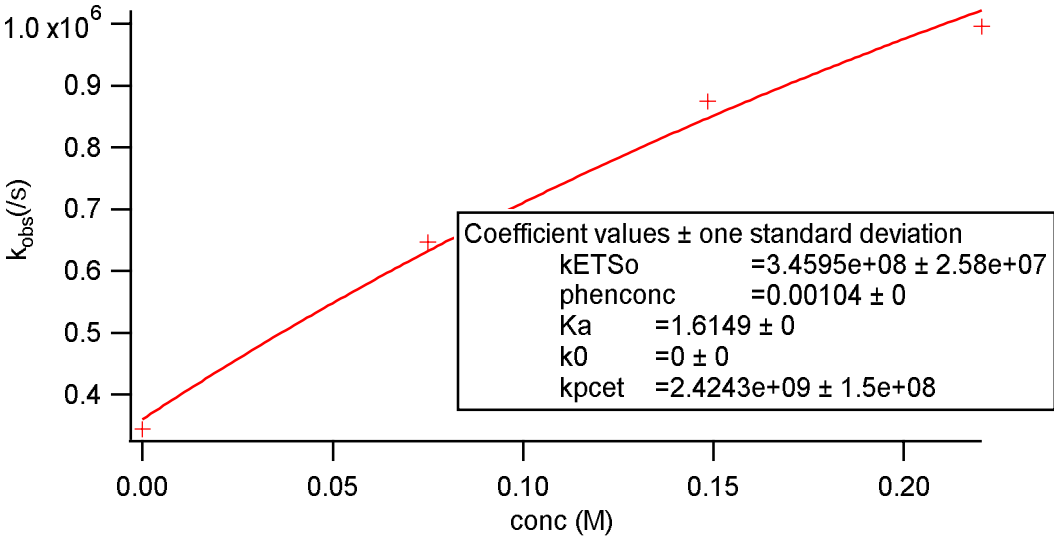

Figure S2.4.4: Observer rate constants for oxidation with $Ru(bpy)_3^{3+}$ as a function of base concentration

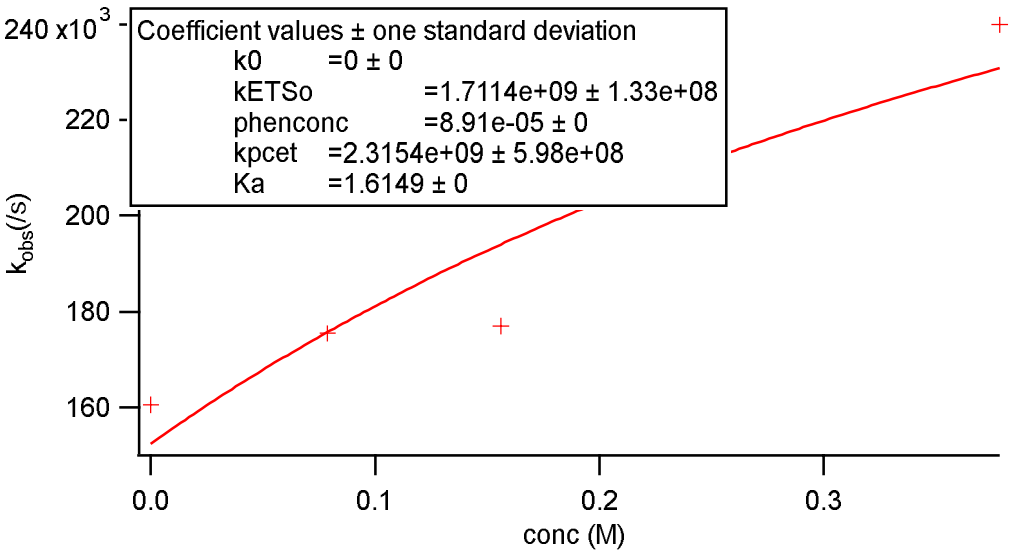

Figure S2.4.5: Observer rate constants for oxidation with $Ru(bpy)_2(deeb)^{3+}$ as a function of base concentration

S3. Determination of $-\Delta G^0_{PCET}$

The driving force of PCET was calculated from the difference in the Bond dissociation free energy (BDFE) of 4-Methoxyphenol and an apparent BDFE calculated from the pKa of the conjugate acid of the proton acceptor and reduction potential of the oxidant, as described by Warren et al.[1] The Bond dissociation enthalpy (BDE) of 4-Methoxyphenol was taken as 81.3 kcal/mol in the gas phase, converted from photoacoustic measurements in benzene by Wayner *et al.*.[2] This was converted to a BDFE in acetonitrile by following the procedure and utilizing values applied by Lymar et al.[3] (supplementary information section S2):

$$BDFE_{gas} = BDE_{gas} - TS^0(H)_{gas}$$

Where $S^0(H)_{gas} = 27.147\ cal/(mol\ K)$.[3,4]

$$BDFE_{MeCN} = BDFE_{gas} + RTln\left(\frac{1 + K_{p-s}}{1 + K_{rad-s}}\right) - \Delta_{gas\rightarrow MeCN}G(H)$$

Where K_{p-s} and K_{rad-s} are hydrogen bonding association constants of the phenol before and after PCET with the solvent (estimated as 110 and 3.3 respectively using Abraham's hydrogen bond acidity and basicity constants)[5], and $\Delta_{gas\rightarrow MeCN}G(H)$ is taken as 3.36 kcal/mol.[3] This resulted in a value of $BDFE_{MeCN} = 78.4\ kcal/mol$.

Apparent BDFEs for the product were calculated with the formula:

$$\frac{BDFE}{(kcal/mol)} = 1.37pK_a + 23.06E^0 + C_G \qquad \text{(eq S3.1)}$$

Where E^0 is the reduction potential of the oxidant vs the $Fc^{(+/0)}$ couple and C_G was taken to be 52.6, as estimated by Lymar et al.[3] The driving force for PCET was calculated by taking the difference between reactant and product BDFEs.

Taking the potential of the $MeOPhenol^{(+./0)}$ couple as 1.18 V vs SCE (see main manuscript) and substracting the $Ru^{(3+/2+)}$ of the oxidant used, the driving force for initial ET ($-\Delta G_{ET1}$) can be calculated. Substracting this from the driving force for PCET leaves $-\Delta G_{PT2}$, (since $\Delta G_{PCET} = \Delta G_{ET1} + \Delta G_{PT2}$). Given ΔG_{PT2} and the pK_a of the corresponding pyridinium acceptors (see main manuscript table 1) a pK_a value of 5.4 for the deprotonated Phenol could be estimated. Lymar et al.[3] estimated the pK_a value of 4-MeOPhenol as 29.2. The energetic coupling between proton and electron (see main manuscript) therefore corresponds to approximately 23.8 pK_a units.

Mechanistic zone diagrams were constructed in the same way as described previously. [6] Rate constants were assumed to be diffusion controlled when they reached the value of 10^{10} /M/s.

S4 Derivation of equation 8

The reaction scheme is described by:

$$4MeOPhenH + B \overset{K_{HB}}{\Longleftrightarrow} [4MeOPhenH \cdots B]$$
$$4MeOPhenH + Ox \xrightarrow{k_{ET}} 4MeOPhenH^{+\cdot} + Ox^{-}$$
$$[4MeOPhenH \cdots B] + Ox \xrightarrow{k_{ETPT_{lim}} + k_{CEPT}} 4MeOPhen^{\cdot} + HB^{+} + Ox^{-}$$

This leads to the following expression for the rate of oxidation:

$$v = -\frac{d[Ox]}{dt} = k_{ET}[4MeOPhen][Ox] + \left(k_{ETPT_{\mathrm{lim}}} + k_{CEPT}\right)[4MeOPhenH \cdots B][Ox]$$

The total phenol and base concentrations correspond to:

$$[4MeOPhen]_0 = [4MeOPhen] + [4MeOPhenH \cdots B]$$
$$[B]_0 = [B] + [4MeOPhenH \cdots B]$$

The rate therefore becomes:

$$v = (k_{ET}[4MeOPhen]_0 - [4MeOPhen \cdots B])[Ox] + \left(k_{ETPT_{\mathrm{lim}}} + k_{CEPT}\right)[4MeOPhenH \cdots B][Ox]$$

The hydrogen bond association constant

$$K_{HB} = \frac{[4MeOPhen \cdots B]}{[4MeoPhenH][B]} = \frac{[4MeOPhen \cdots B]}{([4MeoPhenH]_0 - [4MeOPhen \cdots B])([B]_0 - [4MeOPhen \cdots B])}$$

In the limit where $[B]_0 \gg [4MeOPhenH]_0$:

$$[4MeOPhenH \cdots B] = \frac{K_{HB}[4MeOPhenH]_0[B]_0}{1 + K_{HB}[B]}$$

Substituting this into the rate expression and assuming that $k_{ET} = k_{ETPT_{lim}} = k_{ET(PT)}$leads to:

$$v = k_{ET(PT)}[4MeOPhen][Ox] + k_{CEPT}\frac{K_{HB}[4MeOPhenH]_0[B]_0}{1 + K_{HB}[B]}[Ox]$$

The oxidation can therefore be described with a single rate constant k_{ox} so that:

$$k_{ox}[4MeOPhenH]_0 = k_{ET(PT)}[4MeOPhenH]_0 + k_{CEPT}[4MeOPhenH]_0\frac{K_{HB}[B]_0}{1 + K_{HB}[B]_0}$$

This expression is identical to equation 8 in the main manuscript.

References

1 J. J. Warren, T. A. Tronic and J. M. Mayer, *Chem. Rev.*, 2010, 110, 6961–7001.
2 D. D. M. Wayner, E. Lusztyk, K. U. Ingold and P. Mulder, *J. Org. Chem.*, 1996, 61, 6430–6433.
3 S. V. Lymar, M. Z. Ertem and D. E. Polyansky, *Dalton Trans.*, 2018, 47, 15917–15928.
4 D. D. Wagman, W. H. Evans, V. B. Parker, R. H. Schumm, I. Halow, S. M. Bailey, K. L. Churney and R. L. Nuttall, *J Phys Chem Ref Data*, 1982, 11, suppl-2.
5 M. H. Abraham, *Chem. Soc. Rev.*, 1993, 22, 73–83.
6 R. Tyburski, T. Liu, S. D. Glover and L. Hammarström, *J. Am. Chem. Soc.*, 2021, 143, 560–576.